NONLINEAR AERODYNAMIC ANALYSIS OF BRIDGES UNDER TURBULENT WINDS: THE NEW FRONTIER IN BRIDGE AERODYNAMICS

Xinzhong Chen[1], Ahsan Kareem[1] and Fred L. Haan, Jr.[2]

[1] Department of Civil Engineering and Geological Sciences,
[2] Department of Aerospace and Mechanical Engineering,
University of Notre Dame, Notre Dame, IN 46556-0767, USA

ABSTRACT

Traditionally, the estimation of wind induced buffeting response and analysis of flutter instability have been conducted in the frequency domain utilizing linear approaches. These approaches are limited to linear structures in which nonlinearities in aerodynamic forces are ignored. In this study, a time domain analysis framework for predicting the flutter and buffeting responses of bridges under turbulent winds is presented, in which the nonlinear aerodynamics with respect to the effective angle of incidence is included. The nonlinear unsteady aerodynamic forces are modeled based on the static coefficients, flutter derivatives and admittance functions along with the spanwise correlations at varying angles of incidence. The analysis framework incorporates frequency dependent parameters of unsteady aerodynamic forces by utilizing a rational function approximation technique. A comparison with the conventional linear approach is made through response analysis of a long-span suspension bridge.

KEYWORDS

Flutter, Buffeting, Nonlinear aerodynamics, Bluff body aerodynamics, Time domain simulation, Turbulence, Wind load, Bridge, Random vibration.

INTRODUCTION

The estimation of wind induced buffeting response and analysis of flutter instability have conventionally been conducted in the frequency domain utilizing linear approaches. Longer-span bridges generally require coupled multimode analyses of buffeting and flutter involving aerodynamic coupling effects (e.g., Katsuchi et al. 1999; Chen et al. 2000a). When structural and/or aerodynamic nonlinearities must be included, time domain approaches are most appropriate. In this context, a time domain approach incorporating frequency dependent unsteady aerodynamic forces was proposed by Chen et al. (2000b). A computationally more efficient approach has been proposed using a state-space model of the integrated system including the structure, multi-correlated wind fluctuations, and unsteady buffeting and self-excited forces (Chen and Kareem 2000). These approaches have been applied for linear problems and their effectiveness has been demonstrated.

The aerodynamic forces of most bridge deck sections are highly sensitive to the angle of incidence (e.g., Matsumoto et al. 1998). Even for small levels of turbulence, structural motion and incoming wind fluctuations may vary the effective angle of incidence to such a degree that analysis results may not be realistic without accounting for aerodynamic nonlinearities. In such cases, the accuracy of conventional linear approaches in which the aerodynamic forces are linearized around the mean displaced position warrants further investigation.

Experimental wind tunnel studies have indicated that turbulence can both stabilize and destabilize the flutter instability depending on the geometric configuration of bridge sections and the characteristics of wind fluctuations (e.g., Nakamura 1993). A number of analytical studies using stochastic approaches to randomize the dynamic pressure have been conducted to predict some broad trends in the turbulence-induced changes of the flutter stability (e.g., Lin and Li 1993). Scanlan (1997) addressed the potential mechanism of turbulence on the single torsional flutter due to the spanwise correlation loss of the self-excited forces. Experimental measurements using a rectangular section have indicated that while turbulence results in a slight loss of the spanwise correlation of the self-excited forces, the values remain quite close to unity (Haan 2000). Further experimental investigation on this issue should be addressed including pressure measurements with large spanwise separation. Diana et al. (1999) has analytically investigated the turbulence effects on flutter using a nonlinear aerodynamic force model. This nonlinear model incorporated frequency dependent characteristics by decomposing the total response into components with different frequencies.

In this paper, a time domain analysis framework for predicting the buffeting and flutter responses with nonlinear aerodynamics is presented. In this approach, the nonlinear unsteady aerodynamic forces are modeled based on the static coefficients, flutter derivatives and admittance functions along with the spanwise correlations at varying angles of incidence. Frequency dependent unsteady characteristics have been incorporated by using a rational function approximation technique (Chen et al. 2000). A suspension bridge with a main span of nearly 2000m is used to demonstrate the effectiveness of the proposed approach and to compare with a conventional linear approach.

THEORETICAL BACKGROUND

Nonlinear Unsteady Aerodynamic Forces

Traditional linear aerodynamic force models assume that the variation of effective angle of incidence is small enough that aerodynamic forces can be linearized around the statically deformed position and that the variation of aerodynamic parameters is negligible. For bridge sections with aerodynamic forces that are highly sensitive to angle of incidence, aerodynamic force nonlinearities must be considered. Nonlinearities in the aerodynamic forces arise from a dependence on the effective angle of incidence which consists of contributions from static and dynamic structural motions and from wind fluctuations.

It is reasonable to separate the turbulence into low frequency (large scale) and high frequency (small scale) components corresponding to the frequencies lower than and higher than the lowest natural frequency of the bridge. The effects of low frequency turbulence are considered to contribute to the effective angle of incidence, while the main effects of high frequency turbulence are considered to alter the generation mechanism of aerodynamic forces. High frequency turbulence effects can be modeled by using aerodynamic parameters measured in turbulent flow conditions.

The mean averaged static wind forces, i.e. lift (upward), drag (downwind) and pitching moment (nose-up) components acting on an element of length l are expressed as

$$L_s = -\frac{1}{2}\rho U^2 Bl C_L(\alpha_s); \quad D_s = \frac{1}{2}\rho U^2 Bl C_D(\alpha_s); \quad M_s = \frac{1}{2}\rho U^2 B^2 l C_M(\alpha_s) \qquad (1)$$

where ρ is the air density; U is the mean wind velocity; $B = 2b$ is the bridge deck width; C_L, C_D and C_M are the mean lift, drag and pitching moment coefficients, respectively; and α_s is the time-averaged static angle of the bridge section.

The low frequency components of the aerodynamic forces, which include both self-excited and buffeting force components, can be expressed using the quasi-steady theory–due to the high value of the reduced velocity– in the following nonlinear form:

$$L^l = F_L^l cos\phi^l - F_D^l sin\phi^l - L_s; \qquad D^l = F_L^l sin\phi^l + F_D^l cos\phi^l - D_s; \qquad M^l = F_M^l - M_s \qquad (2)$$

$$F_L^l = -\frac{1}{2}\rho V_r^2 Bl C_L(\alpha_e); \qquad F_D^l = \frac{1}{2}\rho V_r^2 Bl C_D(\alpha_e); \qquad F_M^l = \frac{1}{2}\rho V_r^2 B^2 l C_M(\alpha_e) \qquad (3)$$

$$V_r^2 = (U + u^l - \dot{p}^l)^2 + (w^l + \dot{h}^l + 0.5b\dot{\alpha}^l)^2 \qquad (4)$$

$$\alpha_e = \alpha_s + \alpha^l + \phi^l; \qquad \phi^l = tan^{-1}\left(\frac{w^l + \dot{h}^l + 0.5b\dot{\alpha}^l}{U + u^l - \dot{p}^l}\right) \qquad (5)$$

where u^l and w^l are the longitudinal and vertical wind fluctuations; $h^l(t), p^l(t)$ and $\alpha^l(t)$ are the low frequency components of the dynamic displacements in the vertical, lateral and torsional directions, respectively; α_e is the effective angle of incidence; and the over dot denotes the derivative with respect to time. When the low frequency responses are comparatively small as is the case for long-span bridges, α_e can be approximated as

$$\alpha_e = \alpha_s + tan^{-1}\left(\frac{w^l}{U + u^l}\right) \qquad (6)$$

The high frequency components of the aerodynamic forces are then expressed by a linearization around the effective angle of attack α_e. They can be further separated into self-excited and buffeting force components. Assuming that the self-excited forces within an element are fully correlated spatially, the linearized self-excited forces acting on an element undergoing arbitrary structural motion can be given in terms of a convolution integral as follows for the lift component (e.g., Chen et al. 2000b):

$$L_{se}^h(t) = \frac{1}{2}\rho U^2 l \int_{-\infty}^{t} \left(I_{L_{seh}}(\alpha_e, t - \tau)h^h(\tau) + I_{L_{sep}}(\alpha_e, t - \tau)p^h(\tau)\right.$$

$$\left. + I_{L_{se\alpha}}(\alpha_e, t - \tau)\alpha^h(\tau)\right)d\tau \qquad (7)$$

where $h^h(t), p^h(t)$ and $\alpha^h(t)$ are the high frequency components of the dynamic displacements in the vertical, lateral and torsional directions, respectively; $I_{L_{seh}}, I_{L_{sep}}$ and $I_{L_{se\alpha}}$ are the aerodynamic impulse functions. Unlike the airfoil section in which these aerodynamic impulse functions are related to the Wagner function, bluff bridge sections generally require the use of different functions for the different force components associated separately with lateral, vertical and torsional motions (Scanlan 1992). Analogous formulations hold for the drag and moment components.

The spatial correlation of the buffeting forces should also be considered in the calculation. This results in a reduction of total wind forces on the structure. While it is commonly assumed that the buffeting forces have the same spatial correlation as the approaching wind fluctuations based on strip theory, measurements have suggested that the pressure field may have a higher spanwise correlation. The linearized buffeting forces acting on an element corresponding to arbitrary wind fluctuations can be given in terms of a convolution integral as follows for the lift component (Chen et al. 2000):

$$L_b^h(t) = -\frac{1}{2}\rho U^2 l \int_{-\infty}^{t} \int_{-\infty}^{\tau_2} \left(J_{L_{bu}}(\alpha_e, t - \tau_2)I_{L_{bu}}(\alpha_e, \tau_2 - \tau_1)\frac{u^h(\tau_1)}{U}\right.$$

$$\left. + J_{L_{bw}}(\alpha_e, t - \tau_2)I_{L_{bw}}(\alpha_e, \tau_2 - \tau_1)\frac{w^h(\tau_1)}{U}\right)d\tau_1 d\tau_2 \qquad (8)$$

where u^h and w^h are the wind fluctuations at the center of the element in the longitudinal and vertical directions, respectively; $I_{L_{bu}}$ and $I_{L_{bw}}$ are the aerodynamic impulse functions of buffeting forces representing the unsteady characteristics of buffeting forces on unit length; and $J_{L_{bu}}$ and $J_{L_{bw}}$ indicate the impulse functions representing the spatial correlation characteristics. Analogous formulations hold for the drag and moment components.

For sinusoidal motion and wind fluctuations, the lift components of the self-excited and buffeting forces are commonly expressed in terms of flutter derivatives, admittance functions and joint acceptance functions as:

$$L_{se}^h(t) = \frac{1}{2}\rho U^2 Bl \left(kH_1^* \frac{\dot{h}}{U} + kH_2^* \frac{b\dot{\alpha}}{U} + k^2 H_3^* \alpha + k^2 H_4^* \frac{h}{b} + kH_5^* \frac{\dot{p}}{U} + k^2 H_6^* \frac{p}{b} \right) \tag{9}$$

$$L_b^h(t) = -\frac{1}{2}\rho U^2 Bl \left(2C_L \bar{J}_{L_{bu}} \chi_{L_{bu}} \frac{u}{U} + (C_L' + C_D)\bar{J}_{L_{bw}} \chi_{L_{bw}} \frac{w}{U} \right) \tag{10}$$

where $k = \omega b/U$ is reduced frequency; ω is circular frequency of vibration; $H_i^*(i = 1 \sim 6)$ are frequency dependent flutter derivatives; $\chi_{L_{bu}}$ and $\chi_{L_{bw}}$ denote the aerodynamic transfer functions between fluctuating wind velocities and buffeting forces per unit span (the absolute magnitude of these functions are also referred to as aerodynamic admittance functions); $\bar{J}_{L_{bu}}$ and $\bar{J}_{L_{bw}}$ represent the joint acceptance functions and are the Fourier transform counterparts of the impulse response functions $J_{L_{bu}}$ and $J_{L_{bw}}$, respectively.

The relationship between the aerodynamic impulse response functions, flutter derivatives and admittance functions are given as (Chen et al. 2000).

$$\bar{I}_{L_{seh}} = 2k^2(H_4^* + iH_1^*); \quad \bar{I}_{L_{sep}} = 2k^2(H_6^* + iH_5^*); \quad \bar{I}_{L_{se\alpha}} = 2k^2 b(H_3^* + iH_2^*) \tag{11}$$

$$\bar{I}_{L_{bu}} = 4bC_L\chi_{L_{bu}}; \quad \bar{I}_{L_{bw}} = 2b(C_L' + C_D)\chi_{L_{bw}} \tag{12}$$

where the over bar denotes the Fourier transform operator, and $i = \sqrt{-1}$.

The joint acceptance functions are related to the coherence function coh_r as

$$\bar{J}_r^2 = \frac{1}{l^2} \int_0^l \int_0^l coh_r(x_1, x_2; f) dx_1 dx_2 \quad (r = L_{bu}, L_{bw}) \tag{13}$$

where x_1 and x_2 are the spatial coordinates.

The aerodynamic impulse response functions can be expressed in terms of exponential time-series approximations. For the functions relevant to the self-excited forces, aerodynamic damping and inertia terms can also be included. For example, $I_{L_{seh}}(t)$ is expressed as:

$$\begin{aligned} I_{L_{seh}}(t) &= \left(A_{se,1} + \sum_{j=1}^{m_{se}} A_{se,j+3} \right)\delta(t) + A_{se,2}\frac{b}{U}\dot{\delta}(t) + A_{se,3}\frac{b^2}{U^2}\ddot{\delta}(t) \\ &\quad - \sum_{j=1}^{m_{se}} A_{se,j+3}\frac{d_{se,j}U}{b}exp(-\frac{d_{se,j}U}{b}t) \end{aligned} \tag{14}$$

and for the functions relevant to buffeting forces, for example, $I_{L_{bw}}(t)$ is expressed as:

$$I_{L_{bw}}(t) = 2b(C_L' + C_D)\left(\left(A_{bw,1} + \sum_{j=1}^{m_{bw}} A_{bw,j+3}\right)\delta(t) - \sum_{j=1}^{m_{bw}} A_{bw,j+1}\frac{d_{bw,j}U}{b}exp(-\frac{d_{bw,j}U}{b}t)\right) \tag{15}$$

where $A_{se,1}, A_{se,2}, A_{se,3}, A_{se,j+3}$ and $d_{se,j}$ ($d_j \geq 0; j = 1, ..., m_{se}$) and $A_{bw,1}$ and $d_{bw,j}$ ($d_{bw,j} \geq 0; j = 1, ..., m_{bw}$) are frequency independent coefficients and are functions of angle of incidence. These coefficients can be quantified by fitting the flutter derivatives and admittance function and joint acceptance functions at varying angles of incidence in the frequency domain:

$$2k^2(H_4^* + iH_1^*) = A_{se,1} + (ik)A_{se,2} + (ik)^2 A_{se,3} + \sum_{j=1}^{m_{se}} \frac{(ik)A_{se,j+3}}{ik + d_{se,j}} \tag{16}$$

$$\chi_{L_{bw}} = A_{bw,1} + \sum_{j=1}^{m_{bw}} \frac{(ik)A_{bw,j+1}}{ik + d_{bw,j}} \tag{17}$$

Accordingly, the unsteady frequency dependent aerodynamic forces, for example of $L_{seh}(t)$, can be calculated in the time domain as:

$$L_{seh}(t) = \frac{1}{2}\rho U^2 \left(A_{se,1}h^h(t) + A_{se,2}\frac{b}{U}\dot{h}^h(t) + A_{se,3}\frac{b^2}{U^2}\ddot{h}^h(t) + \sum_{j=1}^{m_{se}} \phi_j^h(t) \right) \tag{18}$$

$$\dot{\phi}_j^h(t) = -\frac{d_{se,j}U}{b}\phi_j^h(t) + A_{se,j+3}\dot{h}^h(t) \qquad (j = 1 \sim m_{se}) \tag{19}$$

where $\phi_j^h(t)$ ($j = 1 \sim m_{se}$) are augmented aerodynamic state vector. Similar formulations for other self-excited force components and buffeting components can be given with analogous definitions and are omitted here for the sake of brevity.

Solution of Equations of Motion

The governing equations of motion of a bridge under wind fluctuations are expressed as

$$\mathbf{M}\ddot{\mathbf{Y}} + \mathbf{C}\dot{\mathbf{Y}} + \mathbf{K}\mathbf{Y} = \mathbf{F}_s + \mathbf{F}^l + \mathbf{F}_{se}^h + \mathbf{F}_b^h \tag{20}$$

where $\mathbf{M}$, $\mathbf{C}$ and $\mathbf{K}$ are the mass, damping and stiffness matrices, respectively; $\mathbf{F}$ is the nodal force vector; subscripts s, se and b represent the static, self-excited and buffeting components; and superscripts l and h represent the low frequency and high frequency components, respectively.

First, the time histories of wind fluctuations with prescribed spectral characteristics at the centers of elements of the bridge must be simulated for the time domain analysis. In this study, an auto-regressive (AR) scheme is used (Chen and Kareem 2000). The power spectral density (PSD) components of the $\mathbf{u}$ and $\mathbf{w}$ vectors used herein are given by the von Karman spectra. Using the simulated wind fluctuations at the center of each element, the low frequency and high frequency components of wind fluctuations can be extracted using fast Fourier transform (FFT) and inverse fast Fourier transform (IFFT) calculations.

At a given mean wind velocity, the mean static deformation of the bridge is calculated by static analysis. This is followed by dynamic response calculations using a Newmark Beta step-by-step integration method. At each time step and at each element the effective angle of incidence is calculated and the associated aerodynamic parameters are determined for the calculation of the buffeting and self-excited forces. An iterative calculation procedure is necessary for both the low frequency and high frequency responses, since the aerodynamic forces depend on the unknown responses. Although iteration is required, the analysis process converges rapidly. For most long span bridges, the low frequency response is negligible, thus the effective angle of attack can be simply evaluated from the low frequency wind fluctuations (Eq. 6). Structural nonlinearities can be also readily incorporated into the analysis. For linear structures, the modal response synthesis technique can be utilized to benefit from the reduction in computational effort afforded by limiting analysis to the selected modes.

APPLICATION

Structural and Aerodynamic Parameters

An example long span suspension bridge with a main span of nearly 2000 m is used to demonstrate the effectiveness of the proposed approach. The bridge deck is a twin-box section. The flutter derivatives H_i^* and A_i^* ($i = 1, 2, 3, 4$) are quantified through wind tunnel testing at varying angles of incidence ranging from -6 deg to 6 deg (Matsumoto et al. 1998). P_1^* is given based on the quasi-steady theory while the other p_i^* coefficients are neglected. Experimental data indicates that A_2^* is highly sensitive to the angle of incidence for this section (Figure 1). For the sake of illustration, only the variation of A_2^* with angle of incidence is considered in this analysis. The admittance and the joint acceptance functions are assumed to be independent of angle of incidence. The admittance functions are given by Davenport's expression for drag, and the Sears function for lift and pitching moment components. The spanwise correlation of buffeting forces is assumed to be same as the corresponding wind fluctuations. The Von Karman spectra is used for the simulation of wind fluctuations with the integral length scales of 80 m and 40 m, intensity of 10 % and 7.5 %, for u- and w-components, respectively.

Results and Discussion

The multimode coupled flutter analysis in frequency domain was conducted by the solution of the complex eigenvalue problem involving first 15 natural modes (Chen et al. 2000). Figure 2 shows the critical flutter velocity at varying mean wind angle of incidence. They were calculated assuming the angle of incidence was uniform in the spanwise direction. Results indicate that this example bridge is very sensitive to the angle of incidence.

Fig. 1 Flutter derivatives A_2^*

Fig. 2 Flutter onset velocity vs angle of incidence

Fig. 3 A realization of wind fluctuation and associated effective angle of incidence (U=60m/s)

For comparison, both linear and nonlinear analysis were conducted at different mean wind velocities. Considering the low frequency component of the response to be negligible, the effective angle of incidence at each element was calculated from the low frequency wind fluctuations (Eq. 6). An example realization of the vertical wind fluctuations and associated effective angle of incidence at the center of the main span at 60 m/s is shown in Fig. 3. The mean static torsional displacement at the main span
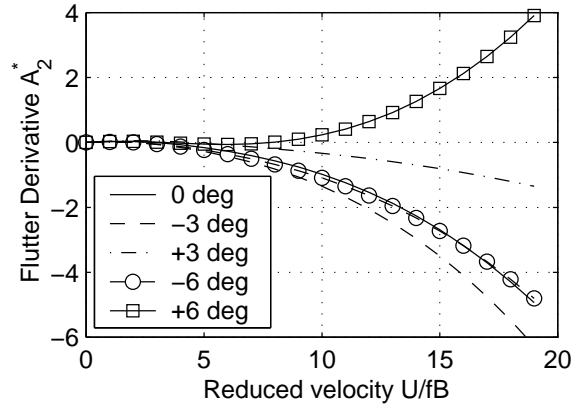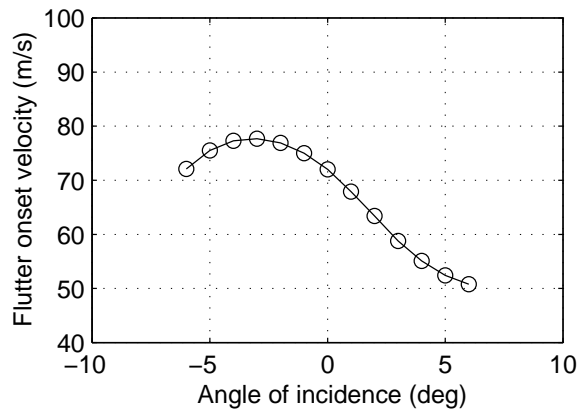
canter is -3.66 deg. The autoregressive model coefficients are determined to generate of time histories of 240 s at an interval of 0.1 s. Figure 4 shows the time histories of the torsional response at the center of main span calculated from the linear and nonlinear analyses at 60 m/s and 80 m/s. Figure 5 shows the comparison of the root-mean-square (RMS) and maximum (MAX) values of torsional displacement at the center of the main span. The nonlinear analysis predicted a significantly larger buffeting response than the linear analysis, and turbulence was found to have a destabilizing effect on flutter stability. These effects of the aerodynamic nonlinearities depend on the magnitude of the effective angle of incidence and the sensitivity of the wind force parameters to the effective angle of incidence. The experimental observation of the changes in the critical flutter velocity due to the turbulence also include the effects of the high frequency turbulence. These effects have not been included in this analysis, but when the aerodynamic force parameters measured in turbulent flow become available, they can readily be used in this analysis framework.

CONCLUSIONS

A time domain approach for predicting the buffeting and flutter responses with aerodynamic nonlinearities was presented. The nonlinear unsteady aerodynamic forces are modeled based on the static coefficients, flutter derivatives and admittance functions along with the spanwise correlations at varying angle of incidence. Their frequency dependent unsteady characteristics have been incorporated by using a rational function approximation technique. Results indicated that analysis with aerodynamic nonlinearity may result in significantly higher buffeting responses than with the linear analysis, and the low frequency turbulence component contributed a destabilizing effect on the flutter stability.

(a) linear case (U=60 m/s)

(b) nonlinear case (U=60 m/s)

(c) linear case (U=80 m/s)

(d) nonlinear case (U=80 m/s)

Fig. 4 Torsional displacement

Fig. 5 Comparison of RMS and Max values at the center of main span

A coordinated experimental investigation is in progress for further validation of the proposed approach. This effort seeks an understanding of turbulence induced modifications of the magnitudes and spanwise coherence of both the buffeting and the self-excited forces. Incorporating such work with measurements of the effective angle and amplitude dependence of the aerodynamic forces will provide an experimental foundation for the analytical work.
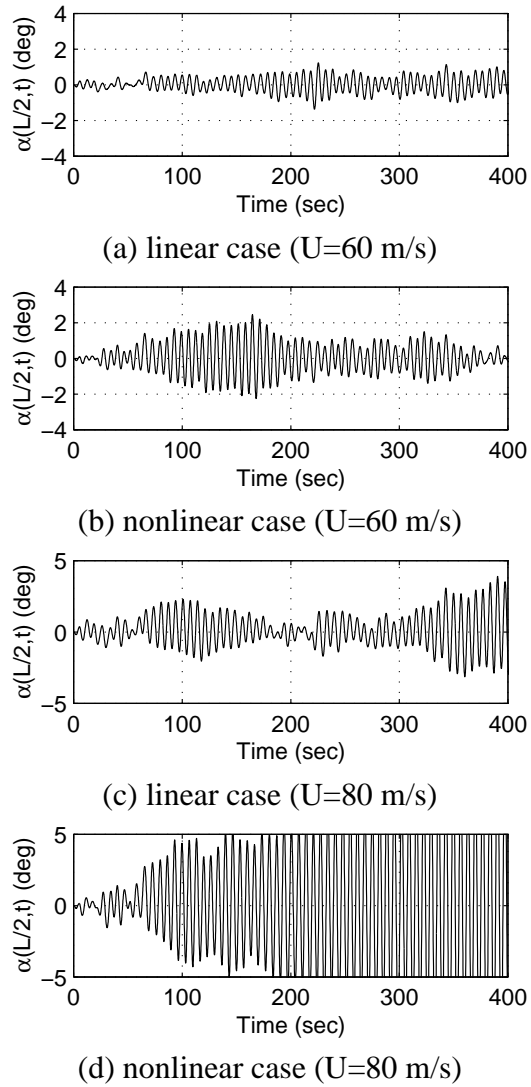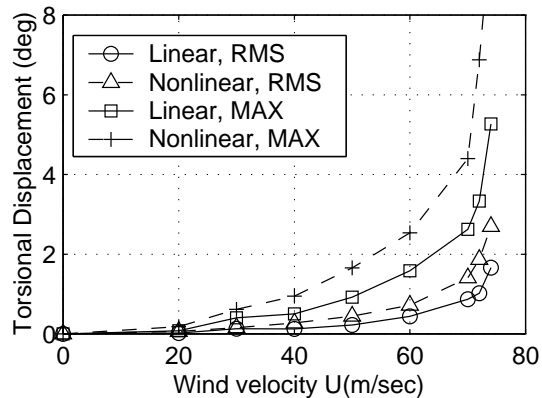
ACKNOWLEDGMENTS

REFERENCES

Chen, X., Kareem, A., Matsumoto, M. (2000a). Coupled flutter and buffeting response of bridges. *Journal of Engineering Mechanics*, ASCE, 126(1), 17-26.

Chen, X., Matsumoto, M., Kareem, A. (2000b). Aerodynamic coupling effects on flutter and buffeting of bridges. *Journal of Engineering Mechanics*, ASCE, 126(1),7-16.

Chen, X., and Kareem, A. (2000). Buffeting response analysis of bridges under multi-correlated winds: a integrated state-space approach. under preparation.

Diana, G., Cheli, F., Zasso, A., Bocciolone, M. (1999). Suspension bridge response to turbulent wind: Comparison of new numerical simulation method results with full scale data. *Wind Engineering into the 21 Century*, Larose & Livesey (eds), Balkema, Rotterdam, 871-878.

Haan, F. L. (2000). The effects of turbulence on the aerodynamics of long-span bridges. A dissertation submitted to the Graduate School of the University of Notre Dame, In partial fulfillment of the requirements of the Degree of Doctor of Philosophy.

Katsuchi, H., Jones, N. P., Scanlan, R. H. (1999). Multimode coupled flutter and buffeting analysis of the Akashi-Kaikyo Bridge. *Journal of Structural Engineering*, ASCE, Vol.125, 60-70.

Lin, Y. K., Li, Q. C. (1993). New stochastic theory for bridge stability in turbulent flow. *Journal of Engineering Mechanics*, ASCE, Vol.119, No.1, 113-127.

Matsumoto, M., Yagi, T., Ishizaki, H., Shitato, H., Chen, X. (1998). Aerodynamic stability of 2-edge girders for cable-stayed bridge. *Proceedings of 15th National Symposium on Wind Engineering*, Japan Association for Wind Engineering, Tokyo, 389-394 (in Japanese).

Nakamura, Y. (1993). Bluff-body aerodynamics and turbulence. *Journal of Wind Engineering and Industrial Aerodynamics*, Vol. 49, 65-78.

Scanlan, R. H. (1992). Problematics in formulation of wind-force models for bridge decks. *Journal of Engineering Mechanics*, ASCE, Vol.119, No.7, 1353-1375.

Scanlan, R. H. (1997). Amplitude and turbulence effects on bridge flutter derivatives. *Journal of Structural Engineering*, Vol. 123, No.2, 232-236.